ARTICLE

doi:10.1038/nature13203

Juno is the egg Izumo receptor and is essential for mammalian fertilization

Enrica Bianchi[1], Brendan Doe[2], David Goulding[3] & Gavin J. Wright[1]

Fertilization occurs when sperm and egg recognize each other and fuse to form a new, genetically distinct organism. The molecular basis of sperm–egg recognition is unknown, but is likely to require interactions between receptor proteins displayed on their surface. Izumo1 is an essential sperm cell–surface protein, but its receptor on the egg has not been described. Here we identify folate receptor 4 (Folr4) as the receptor for Izumo1 on the mouse egg, and propose to rename it Juno. We show that the Izumo1–Juno interaction is conserved within several mammalian species, including humans. Female mice lacking *Juno* are infertile and *Juno*-deficient eggs do not fuse with normal sperm. Rapid shedding of Juno from the oolemma after fertilization suggests a mechanism for the membrane block to polyspermy, ensuring eggs normally fuse with just a single sperm. Our discovery of an essential receptor pair at the nexus of conception provides opportunities for the rational development of new fertility treatments and contraceptives.

Fertilization is the culminating event in sexual reproduction and requires the fusion of haploid sperm and egg to create a new, genetically distinct, diploid organism. Sperm acquire the ability to fertilize the egg within the female reproductive tract by exposing previously concealed receptor proteins onto their surface following the acrosome reaction[1]. Once fertilized, both the oolemma and zona pellucida are biochemically altered, making the egg unreceptive to additional sperm and thereby reducing the chances of creating nonviable polyploid embryos[2]. Several receptor proteins have been implicated in the recognition and/or fusion process[3], but just two significantly affect fertility *in vivo*: Izumo1 on sperm[4], and CD9 on eggs[5–7]. Izumo1 (named after a Japanese marriage shrine) is redistributed to the surface of capacitated sperm[8], and *Izumo1*-deficient male—but not female—mice are infertile because sperm lacking Izumo1 cannot fuse with eggs[4]. Recombinant Izumo1 binds both wild-type and CD9-deficient eggs, suggesting that Izumo1 interacts with an egg receptor other than CD9[9]. Glycophosphatidylinositol (GPI)-anchored receptors on the egg are essential for fertilization because removing them either enzymatically[10] or genetically[11] renders eggs infertile. Despite these advances, the molecular basis of gamete recognition in mammals is unknown; in part, this is due to the scarcity of eggs, the challenges in solubilising membrane-embedded proteins, and the often transient nature of their extracellular interactions[12]. To address these challenges, we have developed techniques to identify low-affinity extracellular interactions and apply them here to investigate sperm–egg recognition in mammals. We now describe the Izumo1 egg receptor as folate receptor 4 (Folr4), a GPI-anchored protein expressed on the egg surface that is essential for female fertility. Because of its role in fertilization and inability to bind folate, we have renamed this protein 'Juno' after the Roman goddess of fertility and marriage.

Juno is the Izumo1 receptor on oocytes

To identify an egg receptor for Izumo1, we expressed the entire ectodomain of mouse Izumo1 in mammalian cells for use as a binding probe. With the expectation that interactions with its extracellular egg receptor would be weak, we oligomerized the Izumo1 ectodomain to increase binding avidity by using a peptide sequence from a cartilage protein that forms pentamers[12] (Extended Data Fig. 1). The avid Izumo1 probe, but not a control protein, bound the oolemma of mouse oocytes (Fig. 1a). To determine the molecular identity of the egg binding partner for Izumo1, we used a mouse oocyte complementary DNA library in an iterative expression cloning approach (Extended Data Fig. 2). In each round of selection, an increasing fraction of transfected cells bound Izumo1 until three independently selected plasmid clones conferred Izumo1 binding (Fig. 1b). All three clones contained the same cDNA, encoding the folate

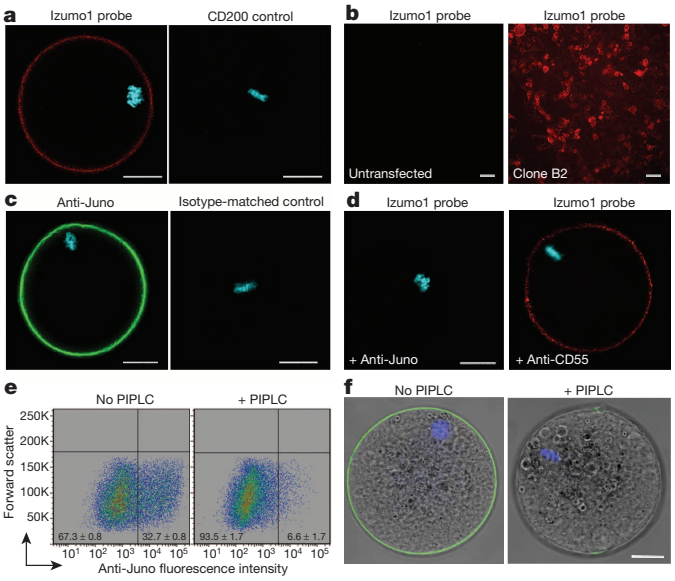

Figure 1 | Juno is the GPI-anchored oocyte surface receptor for Izumo1. **a**, An avid recombinant Izumo1 protein, but not a control, binds the oolemma. **b**, Izumo1 binds HEK293 cells transfected with a *Juno* cDNA (clone B2), but not untransfected controls. **c**, Juno is highly expressed on the oolemma of unfertilized eggs. **d**, Preincubation of eggs with an anti-Juno, but not an anti-CD55 control antibody, blocked binding of recombinant Izumo1 protein. **e**, **f**, Cell-surface Juno was lost after treatment with PIPLC on *Juno*-transfected HEK293 cells (**e**) or eggs (**f**). Images are single optical sections of unfertilized mouse metaphase II eggs; scale bars, 20 μm in **a**, **c**, **d**, **f**; and 10 μm in **b**.

[1]Cell Surface Signalling Laboratory, Wellcome Trust Sanger Institute, Hinxton, Cambridge, CB10 1SA, UK. [2]Mouse Production Team, Wellcome Trust Sanger Institute, Hinxton, Cambridge, CB10 1SA, UK. [3]Electron and Advanced Light Microscopy Suite, Wellcome Trust Sanger Institute, Hinxton, Cambridge, CB10 1SA, UK.

receptor 4 (*Folr4*) gene. Folr4 is one of three folate receptor paralogues in mouse whose main role is thought to involve folate uptake. Folr4 is expressed on $CD4^+CD25^+$ regulatory T cells in mice[13] and is being tested as an anti-tumour therapy[13–15] as well as a mediator of responses to dietary folate[16–18], but no functional role on oocytes has been reported. Using recombinant proteins, we showed that, unlike Folr1 and Folr2, Folr4 was unable to bind to folate (Extended Data Fig. 3a), which was expected given differences in amino acids known to be critical for folate binding[19,20] (Extended Data Fig. 3b). On the basis of these and subsequent findings, we renamed the gene encoding this protein '*Juno*'. Using an anti-Juno monoclonal antibody, we showed that Juno expression matched the binding pattern of the recombinant Izumo probe on ovulated oocytes (Fig. 1c). Preincubating oocytes with the anti-Juno antibody prevented all detectable binding of the Izumo1 probe, demonstrating that Juno is the sole Izumo1 receptor on oocytes (Fig. 1d). Similar to other folate receptor paralogues, the protein sequence of Juno suggested the presence of a carboxy-terminal GPI-anchor site. Given the known importance of oolemmal GPI-linked proteins in fertilization[10,11], we tested whether Juno was tethered to the membrane by a GPI anchor. A large fraction of cell-surface Juno staining was lost after phosphoinositide phospholipase C (PIPLC) treatment of either HEK293 cells transfected with the *Juno* cDNA (Fig. 1e) or oocytes (Fig. 1f), demonstrating that Juno was GPI-anchored, consistent with previous results[21]. Taken together, these data identify Juno as the Izumo1 receptor expressed on oocytes.

Izumo1–Juno interaction is conserved

To show that Izumo1 and Juno interacted directly, and to quantify the biophysical parameters of the interaction, we expressed and purified the entire ectodomain of Juno and measured its binding to Izumo1 using surface plasmon resonance (SPR) (Fig. 2a). Like other extracellular interactions measured using this technique, the interaction was shown to be highly transient with a K_D of ~12 μM (Extended Data Fig. 4). Juno contains a single globular domain[19,20], whereas Izumo1 contains both an immunoglobulin superfamily domain and a unique amino terminus termed the Izumo domain[22]. Consistent with the recent finding that the Izumo domain is sufficient for egg binding[9], we expressed the individual domains of Izumo1 and showed, using an assay designed to detect direct low-affinity extracellular protein interactions called avidity-based extracellular interaction screen (AVEXIS)[23], that it is the Izumo domain that contains both the OBF13 epitope and Juno binding site (Extended Data Fig. 5). Both Izumo1 and Juno belong to small paralogous gene families which, in mouse, contain four and three members, respectively. We expressed the entire ectodomains of Izumo1, 3 and 4 (the Izumo2 paralogue did not express) and used the AVEXIS assay to screen systematically for all possible pairwise interactions with the three Folr paralogues. We observed that only mouse Izumo1 and Juno could interact (Fig. 2b). Clearly identifiable *Izumo1* and *Juno* orthologues exist in all sequenced mammalian genomes, including marsupials. To determine whether the interaction was conserved within mammals, we expressed the entire ectodomains of both Izumo1 and Juno orthologues from humans, pig (*Sus scrofa*) and opossum (*Monodelphis domestica*) and assessed binding using the AVEXIS assay. Clear binding between the orthologues was observed, demonstrating that the interaction is conserved within mammals (Fig. 2c).

Juno is essential for fertilization

To assess the role of Juno in fertilization, we first added an anti-Juno monoclonal antibody that blocks the Izumo–Juno interaction (Fig. 1d) into *in vitro* fertilization (IVF) assays. The anti-Juno antibody potently prevented fertilization (Fig. 3a), with no detectable fertilization events even when used at concentrations as low as 0.1 μg ml^{-1} (Extended Data Fig. 6). Using similar approaches, previous research in this area has identified promising candidates for sperm–egg recognition that, when genetically deleted, have been shown to be dispensable for fertilization[3]. To determine whether *Juno* was essential for fertilization, we created *Juno*-deficient mice using embryonic stem cells disrupted at the *Folr4*

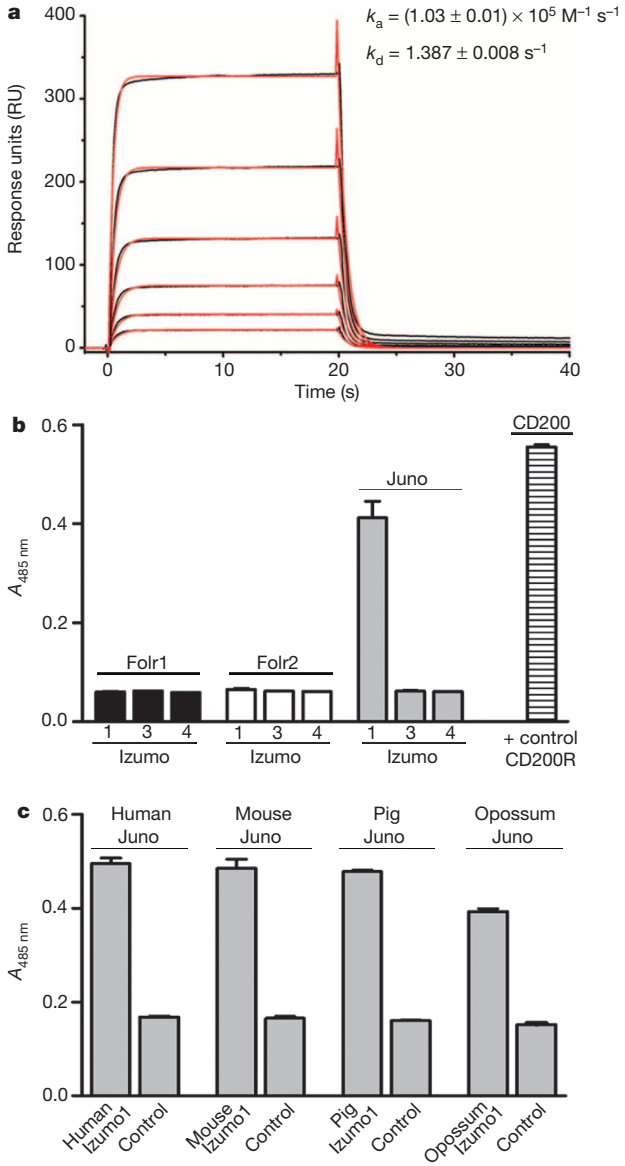

Figure 2 | The Izumo1–Juno interaction is direct, transient and conserved across mammals. **a**, Biophysical analysis of the Izumo1–Juno interaction using SPR. Serial dilutions of purified, soluble Juno were injected over immobilised Izumo1, and kinetic parameters derived from a 1:1 Langmuir binding model (red lines). **b**, Binding specificity within the paralogues of the mouse Izumo and Folr families: only Juno (Folr4) bound Izumo1. **c**, The Izumo1–Juno interaction is conserved across mammals. AVEXIS was used for binding analysis in **b** and **c** using recombinant Folr/Juno proteins as preys and Izumo proteins as baits; control bait in **c** was CD4. All bar charts show mean ± s.e.m.; $n = 3$.

locus using a gene trap allele: *Folr4*$^{tm1a(KOMP)Wtsi}$ (Extended Data Fig. 7). Both *Juno*$^{-/-}$ male and female mice developed indistinguishably from wild-type controls, showing normal rates of growth and morphology and were overtly healthy. Whereas *Juno*$^{-/-}$ male and *Juno*$^{+/-}$ female mice were fertile, by contrast, *Juno*$^{-/-}$ females failed to produce any litters during three months of continuous mating with wild-type males of proven fertility (Fig. 3b). Female *Juno*$^{-/-}$ mice exhibited natural mating behaviours, as assessed by vaginal plug formation and the presence of motile sperm in the reproductive tract when paired with fertile wild-type males. *Juno*$^{-/-}$ females responded to hormone treatment by ovulating morphologically normal eggs at numbers that did not significantly differ from wild-type. *Juno*$^{-/-}$ eggs recovered at embryonic day 0.5 after superovulation and natural mating were not fertilized and had more sperm within their perivitelline space compared to wild-type eggs, demonstrating that the zona pellucida of *Juno*$^{-/-}$ eggs could be

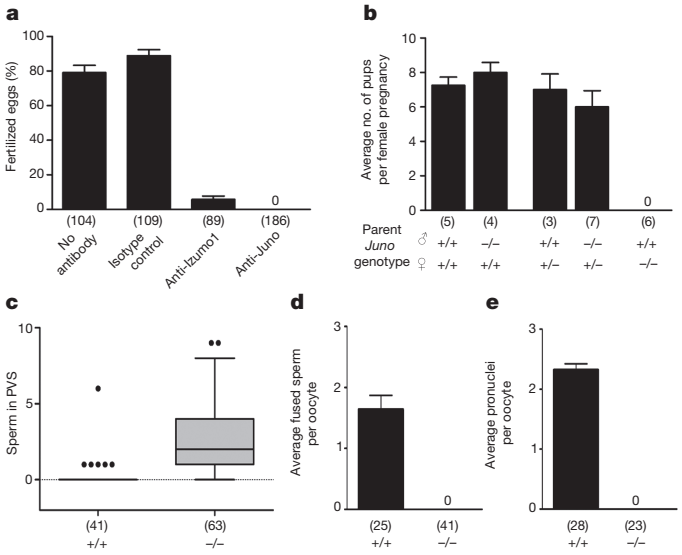

Figure 3 | *Juno* is essential for female fertility. **a**, An anti-Juno monoclonal antibody potently blocked *in vitro* fertilization; anti-Izumo1 is shown for comparison. **b**, Female *Juno*$^{-/-}$ mice are infertile. Continuous mating of *Juno*$^{-/-}$ female mice to proven wild-type males for 3 months did not result in any pups. **c**, Greater numbers of sperm were observed in the perivitelline space (PVS) of eggs from superovulated *Juno*-deficient (−/−) mice relative to wild-type (+/+). **d**, **e**, Zona-free *Juno*$^{-/-}$ eggs do not fuse with wild-type sperm *in vitro*. Sperm were added to Juno-deficient (−/−) and wild-type (+/+) eggs and fused sperm quantified after two hours (**d**), or pronuclei after six hours (**e**). All bar charts show mean ± s.e.m.; numbers in parentheses are total number of eggs (**a**, **c**, **d**, **e**) or number of mating pairs (**b**).

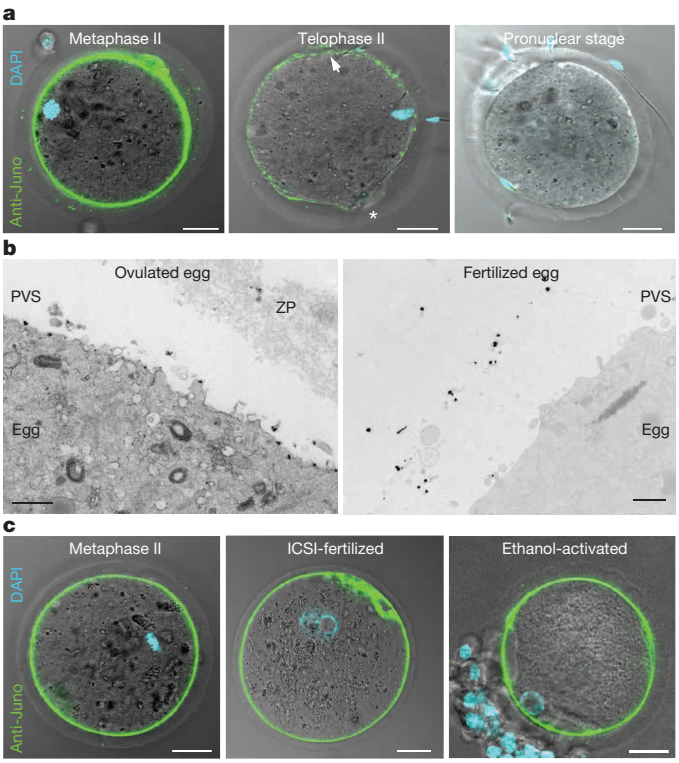

Figure 4 | Juno is rapidly shed from the oolemma of normally fertilized eggs, but not ICSI-fertilized or parthenogenetically activated eggs. **a**, Cell-surface Juno rapidly becomes undetectable after fertilization. Juno (green) is expressed on ovulated metaphase II eggs, but is barely evident at telophase II and undetectable on pronuclear-stage zygotes. Arrow and asterisk indicate sites of first and second polar body extrusion, respectively; chromosomes are not within the plane of focus. **b**, Immunogold electron microscopy localized Juno primarily to the oolemma in unfertilized, ovulated eggs, but was redistributed to vesicles within the perivitelline space within 1 h after fertilization. ZP, zona pellucida. **c**, Eggs fertilized by ICSI or parthenogenetically activated retain oolemmal Juno staining until at least the pronuclear stage, as shown. Nuclei/pronuclei were visualized with DAPI (blue). Images show representative eggs from three independent experiments. Scale bars represent 20 μm (**a**, **c**) and 1 μm (**b**).

penetrated by wild-type sperm *in vivo*, which then either did not bind or fuse with the oolemma (Fig. 3c). To investigate this further, we removed the zona pellucida from *Juno*$^{-/-}$ eggs and found that they could not be fertilized with wild-type sperm in IVF assays, as assessed by counting the number of fused sperm and formed pronuclei per egg (Fig. 3d, e). This is consistent with a role for the Izumo1–Juno interaction in sperm–egg adhesion or fusion. To distinguish between these possibilities, normally non-fusing HEK293 cells were separately transfected with plasmids encoding either *Juno* or *Izumo1* cDNAs and mixed. No syncytia were observed in the mixed cultures, indicating that the interaction is not sufficient for cell fusion (Extended Data Fig. 8a). Furthermore, acrosome-reacted normal sperm did not bind as efficiently to zona-free Juno-deficient eggs as wild-type controls (Extended Data Fig. 8b). Together, these findings indicate that the Izumo1–Juno interaction is a necessary adhesion event between sperm and egg that is required for fertilization.

Juno is rapidly shed after fertilization

After fertilization, oocytes become largely refractory to further sperm fusion events to prevent the creation of nonviable polyploid embryos due to polyspermy. This is achieved through both a relatively slow-acting (>1 h) hardening of the zona pellucida caused by the action of enzymes released from cortical granules after egg activation, and a faster-acting block involving biochemical changes in the oolemmal membrane. In broadcast-spawning frogs and aquatic invertebrates, the membrane block to polyspermy is very fast (a few seconds to minutes) and is achieved by electrically depolarizing the oolemma[24]. In mammals, the membrane block occurs over a longer timeframe (30–45 min), and despite being first described 60 years ago, its mechanistic basis remains a mystery[2]. Given the essential role of Juno in fertilization, we explored the role it might play in establishing the membrane block to polyspermy. Interestingly, cell-surface Juno was rapidly lost after fertilization, being only weakly detectable in zona-intact fertilized eggs at telophase II and undetectable at the pronuclear stage (Fig. 4a). Similarly, Juno was barely detectable on anaphase-II-stage zona-free oocytes, approximately 30 to 40 min after fertilization (Extended Data Fig. 9). Folate receptors are known to take up extracellular dietary folate by endocytosis[25] and we therefore used immunogold electron microscopy to determine the subcellular localization of Juno following fertilization. Surprisingly, we observed that Juno was not internalised after fertilization but present in extracellular vesicles, presumably derived from the microvillus-rich oolemma that undergoes significant architectural changes upon fertilization[26] (Fig. 4b). Some methods of fertilization, such as intracytoplasmic sperm injection (ICSI) and parthenogenetic activation, do not lead to the establishment of an effective membrane polyspermic block[2]. Consistent with a role for Juno in the membrane block to polyspermy, eggs fertilized either by ICSI, or parthenogenetically activated by ethanol, did not lose cell-surface expression of Juno (Fig. 4c). The rapid shedding of Juno from the egg membrane within vesicles after fertilization therefore provides a possible mechanism for the membrane block to polyspermy in mammalian eggs.

Discussion

To our knowledge, the discovery of Juno as the binding partner for Izumo1 identifies these proteins as the first cell-surface receptor pair essential for gamete recognition in any organism. Importantly, both female *Juno* and male *Izumo1*-deficient mice are infertile, suggesting that the interaction is essential for normal fertilization. Comparing our findings with recent advances in the molecular understanding of cellular fusion in other biological contexts suggests that the Izumo1–Juno interaction performs a necessary adhesion step rather than acting as a

membrane 'fusogen'. Unlike established fusogens such as the EFF-1 and AFF-1 proteins[27] or syncytins[28], that are sufficient for fusion, Juno and Izumo1 do not induce the formation of syncytia when ectopically expressed on neighbouring non-fusing cells. Essential adhesion processes are required in other cellular fusion systems such as myofibre formation in both *Drosophila*[29] and vertebrates[30], suggesting that membrane fusion requires the action of other membrane proteins such as myomaker[31]. The expected but remarkably low *in vitro* binding affinity between soluble monomeric Juno and Izumo1 suggests that local clustering of Juno within the oolemma is important to ensure a sufficiently high binding avidity for productive interactions, a role that could be performed by the tetraspanin CD9. Tetraspanins are known to organize other membrane proteins within microdomains[32], and quantitative differences in sperm adhesion to CD9-deficient eggs have been reported[33]. This may also explain why female mice lacking CD9 have reduced fertility[5–7], unlike Juno-deficient mice which are completely infertile. The ability of CD9 to organize Juno within the oolemma may be indirect because oocytes lacking CD9 have an altered membrane architecture[34,35].

Several pieces of evidence point to the rapid loss of Juno from the egg membrane after fertilization as the mechanistic basis for the membrane block to polyspermy in mammals. First, cell-surface Juno is essential for fertilization; second, it is undetectable on the oolemma approximately 40 min after fertilization, in excellent agreement with the timing of the membrane block[36]; third, the membrane block is both a graded response[37] and associated with the loss of sperm binding sites[38], consistent with the gradual loss of a surface receptor; and fourth, surface Juno expression is not lost in ICSI-fertilized or parthenogenetically-activated eggs that do not form an effective membrane block[39]. One further possibility is that because Juno is shed as vesicles after fertilization, this creates a zone of 'decoy eggs' confined within the perivitelline space that could bind to and efficiently neutralise incoming acrosome-reacted sperm to increase the potency of the sperm block. In conclusion, our discovery of an extracellular receptor pair essential for fertilization provides a focus for the rational development of novel contraceptives and fertility treatments.

METHODS SUMMARY

Transgenic mice. All animal experiments were performed in accordance with local ethical and UK Home Office regulations. *Juno*-deficient mice (*Folr4*$^{tm1a(KOMP)Wtsi}$) were generated by the Sanger Institute Mouse Genetics Project from *Folr4*-targeted mouse embryonic stem cells as part of the International Knockout Mouse Consortium, essentially as described[40]. Acrosome reporter mice (B6;B6C3-Tg(Acro3-EGFP)01Osb)[41], where the enhanced green fluorescent protein labels acrosome-intact sperm, were obtained from the RIKEN BioResource Centre. Wild-type eggs were obtained from BJCB strain mice for IVF, parthenogenetic activation and ICSI procedures. Sibling C57BL6/6N wild-types were used as controls in all other experiments.

***In vitro* fertilization assays and ICSI.** IVF and ICSI were performed as previously described[42,43]. Eggs were collected from hormone-primed females and sperm were capacitated before mixing. Fertilization and egg activation were assessed by staining sperm DNA and egg chromosomes. Acrosome-reacted sperm were identified using Acro3–EGFP reporter mice. Juno expression analysis was performed by immunofluorescence and images acquired with a Leica SP5 confocal microscope. Fertilization was quantified by counting decondensed sperm heads in the egg cytoplasm, or scoring the number of pronuclei.

Recombinant protein production and expression cloning. All protein expression constructs were made by gene synthesis (GeneArt). Protein production, purification, AVEXIS assays and SPR were performed essentially as described[23,44]. The *Juno* cDNA was identified by iterative rounds of selection by transfecting adherent HEK293T cells with a commercially available mouse oocyte cDNA library, NIH_MGC_257_N (Express Genomics, USA).

Online Content Any additional Methods, Extended Data display items and Source Data are available in the online version of the paper; references unique to these sections appear only in the online paper.

Received 9 January; accepted 5 March 2014.
Published online 16 April 2014.

1. Okabe, M. The cell biology of mammalian fertilization. *Development* **140,** 4471–4479 (2013).
2. Gardner, A. J. & Evans, J. P. Mammalian membrane block to polyspermy: new insights into how mammalian eggs prevent fertilisation by multiple sperm. *Reprod. Fertil. Dev.* **18,** 53–61 (2006).
3. Ikawa, M., Inoue, N., Benham, A. M. & Okabe, M. Fertilization: a sperm's journey to and interaction with the oocyte. *J. Clin. Invest.* **120,** 984–994 (2010).
4. Inoue, N., Ikawa, M., Isotani, A. & Okabe, M. The immunoglobulin superfamily protein Izumo is required for sperm to fuse with eggs. *Nature* **434,** 234–238 (2005).
5. Le Naour, F., Rubinstein, E., Jasmin, C., Prenant, M. & Boucheix, C. Severely reduced female fertility in CD9-deficient mice. *Science* **287,** 319–321 (2000).
6. Miyado, K. *et al.* Requirement of CD9 on the egg plasma membrane for fertilization. *Science* **287,** 321–324 (2000).
7. Kaji, K. *et al.* The gamete fusion process is defective in eggs of Cd9-deficient mice. *Nature Genet.* **24,** 279–282 (2000).
8. Satouh, Y., Inoue, N., Ikawa, M. & Okabe, M. Visualization of the moment of mouse sperm-egg fusion and dynamic localization of IZUMO1. *J. Cell Sci.* **125,** 4985–4990 (2012).
9. Inoue, N. *et al.* Molecular dissection of IZUMO1, a sperm protein essential for sperm-egg fusion. *Development* **140,** 3221–3229 (2013).
10. Coonrod, S. A. *et al.* Treatment of mouse oocytes with PI-PLC releases 70-kDa (p/ 5) and 35- to 45-kDa (p/ 5.5) protein clusters from the egg surface and inhibits sperm-oolemma binding and fusion. *Dev. Biol.* **207,** 334–349 (1999).
11. Alfieri, J. A. *et al.* Infertility in female mice with an oocyte-specific knockout of GPI-anchored proteins. *J. Cell Sci.* **116,** 2149–2155 (2003).
12. Wright, G. J. Signal initiation in biological systems: the properties and detection of transient extracellular protein interactions. *Mol. Biosyst.* **5,** 1405–1412 (2009).
13. Yamaguchi, T. *et al.* Control of immune responses by antigen-specific regulatory T cells expressing the folate receptor. *Immunity* **27,** 145–159 (2007).
14. Teng, M. W. *et al.* Multiple antitumor mechanisms downstream of prophylactic regulatory T-cell depletion. *Cancer Res.* **70,** 2665–2674 (2010).
15. Liang, S. C., Moskalenko, M., Van Roey, M. & Jooss, K. Depletion of regulatory T cells by targeting folate receptor 4 enhances the potency of a GM-CSF-secreting tumor cell immunotherapy. *Clin. Immunol.* **148,** 287–298 (2013).
16. Kunisawa, J., Hashimoto, E., Ishikawa, I. & Kiyono, H. A pivotal role of vitamin B9 in the maintenance of regulatory T cells *in vitro* and *in vivo*. *PLoS ONE* **7,** e32094 (2012).
17. Kinoshita, M. *et al.* Dietary folic acid promotes survival of Foxp3$^+$ regulatory T cells in the colon. *J. Immunol.* **189,** 2869–2878 (2012).
18. Salbaum, J. M., Kruger, C. & Kappen, C. Mutation at the folate receptor 4 locus modulates gene expression profiles in the mouse uterus in response to periconceptional folate supplementation. *Biochim. Biophys. Acta* **1832,** 1653–1661 (2013).
19. Chen, C. *et al.* Structural basis for molecular recognition of folic acid by folate receptors. *Nature* **500,** 486–489 (2013).
20. Wibowo, A. S. *et al.* Structures of human folate receptors reveal biological trafficking states and diversity in folate and antifolate recognition. *Proc. Natl Acad. Sci. USA* **110,** 15180–15188 (2013).
21. Jia, Z. *et al.* A novel splice variant of FR4 predominantly expressed in CD4$^+$CD25$^+$ regulatory T cells. *Immunol. Invest.* **38,** 718–729 (2009).
22. Ellerman, D. A. *et al.* Izumo is part of a multiprotein family whose members form large complexes on mammalian sperm. *Mol. Reprod. Dev.* **76,** 1188–1199 (2009).
23. Bushell, K. M., Sollner, C., Schuster-Boeckler, B., Bateman, A. & Wright, G. J. Large-scale screening for novel low-affinity extracellular protein interactions. *Genome Res.* **18,** 622–630 (2008).
24. Jaffe, L. A. Fast block to polyspermy in sea urchin eggs is electrically mediated. *Nature* **261,** 68–71 (1976).
25. Sabharanjak, S. & Mayor, S. Folate receptor endocytosis and trafficking. *Adv. Drug Deliv. Rev.* **56,** 1099–1109 (2004).
26. Jackowski, S. & Dumont, J. N. Surface alterations of the mouse zona pellucida and ovum following *in vivo* fertilization: correlation with the cell cycle. *Biol. Reprod.* **20,** 150–161 (1979).
27. Podbilewicz, B. *et al.* The *C. elegans* developmental fusogen EFF-1 mediates homotypic fusion in heterologous cells and *in vivo*. *Dev. Cell* **11,** 471–481 (2006).
28. Mi, S. *et al.* Syncytin is a captive retroviral envelope protein involved in human placental morphogenesis. *Nature* **403,** 785–789 (2000).
29. Abmayr, S. M. & Pavlath, G. K. Myoblast fusion: lessons from flies and mice. *Development* **139,** 641–656 (2012).
30. Powell, G. T. & Wright, G. J. Jamb and Jamc are essential for vertebrate myocyte fusion. *PLoS Biol.* **9,** e1001216 (2011).
31. Millay, D. P. *et al.* Myomaker is a membrane activator of myoblast fusion and muscle formation. *Nature* **499,** 301–305 (2013).
32. Hemler, M. E. Tetraspanin functions and associated microdomains. *Nature Rev. Mol. Cell Biol.* **6,** 801–811 (2005).
33. Jégou, A. *et al.* CD9 tetraspanin generates fusion competent sites on the egg membrane for mammalian fertilization. *Proc. Natl Acad. Sci. USA* **108,** 10946–10951 (2011).
34. Runge, K. E. *et al.* Oocyte CD9 is enriched on the microvillar membrane and required for normal microvillar shape and distribution. *Dev. Biol.* **304,** 317–325 (2007).
35. Żyłkiewicz, E., Nowakowska, J. & Maleszewski, M. Decrease in CD9 content and reorganization of microvilli may contribute to the oolemma block to sperm penetration during fertilization of mouse oocyte. *Zygote* **18,** 195–201 (2010).
36. Wolf, D. P. The block to sperm penetration in zona-free mouse eggs. *Dev. Biol.* **64,** 1–10 (1978).
37. Gardner, A. J., Williams, C. J. & Evans, J. P. Establishment of the mammalian membrane block to polyspermy: evidence for calcium-dependent and -independent regulation. *Reproduction* **133,** 383–393 (2007).

38. Horvath, P. M., Kellom, T., Caulfield, J. & Boldt, J. Mechanistic studies of the plasma membrane block to polyspermy in mouse eggs. *Mol. Reprod. Dev.* **34,** 65–72 (1993).
39. Wortzman-Show, G. B., Kurokawa, M., Fissore, R. A. & Evans, J. P. Calcium and sperm components in the establishment of the membrane block to polyspermy: studies of ICSI and activation with sperm factor. *Mol. Hum. Reprod.* **13,** 557–565 (2007).
40. Skarnes, W. C. *et al.* A conditional knockout resource for the genome-wide study of mouse gene function. *Nature* **474,** 337–342 (2011).
41. Nakanishi, T. *et al.* Real-time observation of acrosomal dispersal from mouse sperm using GFP as a marker protein. *FEBS Lett.* **449,** 277–283 (1999).
42. Nagy, A., Gertsenstein, M., Vintersten, K. & Behringer, R. *Manipulating the Mouse Embryo: A Laboratory Manual* 3rd edn (Cold Spring Harbor Laboratory Press, 2003).
43. Kimura, Y. & Yanagimachi, R. Intracytoplasmic sperm injection in the mouse. *Biol. Reprod.* **52,** 709–720 (1995).
44. Sun, Y., Gallagher-Jones, M., Barker, C. & Wright, G. J. A benchmarked protein microarray-based platform for the identification of novel low-affinity extracellular protein interactions. *Anal. Biochem.* **424,** 45–53 (2012).

Acknowledgements This work was supported by the Wellcome Trust grant number 098051. *Juno*-deficient mice were generated by the Sanger Institute Mouse Genetics Project. We thank W. Skarnes and J. Bussell for advice on transgenic mice; J. Kerr for construct design; A. Bradley and L. Jovine for helpful comments on the manuscript; and M. Okabe and N. Inoue for the OBF13 antibody.

Author Contributions E.B. and G.J.W. conceived the project, designed and analysed the experiments, and wrote the manuscript. E.B. performed all experiments with technical help from B.D. (ICSI) and D.G. (electron microscopy).

Author Information Reprints and permissions information is available at www.nature.com/reprints. The authors declare no competing financial interests. Readers are welcome to comment on the online version of the paper. Correspondence and requests for materials should be addressed to G.J.W. (gw2@sanger.ac.uk).

METHODS

Generation and breeding of transgenic mice. All animal experiments were performed in accordance with local ethical and UK Home Office regulations. *Juno*-deficient mice contain a 'knockout-first' allele targeted to the *Juno*/*Folr4* genomic locus named *Folr4*$^{tm1a(KOMP)Wtsi}$ and were obtained from the Knockout Mouse Project resource (KOMP-CSD ID:28054)[40]. Briefly, mouse embryonic stem cells derived from C57BL/6N mice containing the correctly targeted *Juno*/*Folr4* locus were injected into mouse blastocysts and transplanted in pseudopregnant mice to generate chimaeras. Highly (80–90%) chimaeric males were mated with C57BL/6NTac females and germ line transmission of the targeted allele confirmed by PCR. The tm1a heterozygous mice were bred to obtain homozygous mice and sibling C57BL6/6N wild types were used as controls, as appropriate. Animals were genotyped using DNA extracted from ear biopsies using TaqMan Sample-to-SNP Kit and used as the template for short range PCR. Wild-type and mutant alleles were amplified using the same forward primer: Juno-F: 5′-CACTGTCTGATGAGGGC CAG-3′ and two different reverse primers: Juno-R 5′-AGAGCCCAGGAGGGAA CAACCTC-3′ for the wild-type allele, Cas-R 5′-TCGTGGTATCGTTATGCGCC-3′ for the mutant allele. To rule out the possibility that the fertility defect was due to closely linked secondary mutations, a second colony of *Juno*-deficient mice were created using an independent embryonic stem cell clone targeted with the same gene trapping allele: *Folr4*$^{tm2a(KOMP)Wtsi}$ (KOMP-CSD ID:28055); homozygous *Juno*$^{tm2a/tm2a}$ mutant females were also infertile. The fertility defect was rescued by reverting the *Juno*^{tm2a} allele essentially to a wild-type 'floxed' *Juno*^{tm2c} allele by crossing to mice that constitutively and ubiquitously express the FLPe-recombinase from the *Rosa26* locus (*Rosa26*^{Fki} mice). Revertant homozygous (*Juno*$^{tm2c/tm2c}$) eggs were fertile in IVF assays (Extended Data Fig. 7). Male and female fertility was assessed in long-term mating tests by pairing homozygous and heterozygous *Juno* adult transgenic mice with wild-type animals of proven fertility and the number of pups was monitored continuously for three months. *In vivo* fertilization was assessed by recovered oocytes from ampullae at embryonic day 0.5, fixed in 2% formalin, and stained with DAPI to quantify the number of fertilized eggs. Sperm in the perivitelline space were quantified using a Leica SP5/DM6000 confocal microscope. Acro3–EGFP, acrosome reporter mice (B6;B6C3-Tg(Acro3-EGFP)01Osb)[41] were obtained from the RIKEN BioResource Centre.

***In vitro* fertilization.** *In vitro* fertilization was performed essentially as described[42]. Briefly, female mice were superovulated by injecting 5 IU of pregnant mare serum gonadotropin and 5 IU of human chorionic gonadotropin 48 h later. Wild-type eggs were collected from the BJCB strain (CBA <Wtsi>;C57BL/6J-Jax F1) for *in vitro* fertilization, ICSI, parthenogenetic activation and antibody staining. Eggs recovered 13 h after hCG were freed from cumulus cells by a brief incubation in EmbryoMax M2 medium supplemented with hyaluronidase (Millipore), washed in M2 medium (Sigma) and where indicated, the zona pellucida was removed by a rapid treatment with EmbryoMax acidic Tyrode's solution (Millipore). Sperm were collected from the caudae epididymes of adult (>8 week-old) male mice and cultured for 1 h in HTF medium. *In vitro* fertilization assays were performed using groups of 30 to 60 eggs which were inseminated in 100-µl drops of HTF medium containing 1×10^5–2×10^5 sperm. Eggs were fixed at the indicated stage for 20 min with 2% formalin in M2, and fertilization quantified by visualization of decondensed sperm head nuclei or pronuclei formation. For antibody blocking experiments, anti-Juno/Folr4 monoclonal antibody was added to zona-free eggs and incubated for ten minutes before adding sperm. Parthenogenetic activation of eggs was achieved by a six minute incubation in 7% ethanol, followed by washes in M2 medium. Eggs were then cultured for five hours to assess completion of the second meiotic division and formation of the female pronucleus.

Intracytoplasmic sperm injection. Intracytoplasmic sperm injection (ICSI) was carried out as described[43] with some modifications. Epididymes were placed into 1 ml 37 °C HEPES-buffered-CZB media (H-CZB) in an Eppendorf tube and three to four incisions made to release sperm and incubated at 37 °C for 30–45 min to allow sperm to 'swim up'. Injections were performed by first applying one or more piezo pulses to 'drill' through the zona pellucida (piezo settings, intensity: 20, speed: 10, pulse: infinity) then a single piezo pulse was applied (piezo settings, intensity: 1–3, speed: 1–3, pulse: 1–3) to gently break the oolemma; finally, a single sperm head previously separated from the mid-piece and tail by piezo (piezo settings, intensity: 20, speed 10, pulse: infinity) was deposited immediately into the oocyte. Surviving oocytes were placed into a 100 µl equilibrated drop of KSOM medium after 'resting' for 10 min at room temperature. Eppendorf micromanipulators, microinjectors and a piezo actuator were used for the ICSI procedure (NK2 Transferman, Cell tram vario, Cell tram air and Piezoexpert).

Recombinant protein production. The regions encoding the entire extracellular domains of Izumo1 and Juno orthologues were made by gene synthesis and codon optimised for expression in human cells (GeneArt). Protein sequences for Izumo1 orthologues were: mouse, *Mus musculus* (Uniprot accession number Q9D9J7); human, *Homo sapiens* (Q8IYV9); pig, *Sus scrofa* (F1RIQ7) and opossum, *Monodelphis domestica* (H9H653). Juno/Folr4 were: mouse (Q9EQF4); human (A6ND01); pig (F1STK4); and opossum (F7AHC3). Mouse Izumo and Juno paralogues were: Izumo2 (Q9DA16), Izumo3 (A6PWV3), Izumo4 (D3Z690), Folr1 (P35846), and Folr2 (Q05685). The rat CD200 and CD200R were used for positive controls as described[44]. All ectodomains were flanked by unique NotI and AscI sites that were used to clone them into protein expression vectors that encoded either biotinylated 'baits' or pentameric Flag-tagged 'preys'[45]. An expression construct produced in exactly the same manner containing the Izumo2 paralogue did not produce any protein in several independent transfections. The Izumo and Ig-like domain fragments were amplified from the entire ectodomain construct by PCR and either cloned into the normal biotinylated 'bait' vector (Izumo domain) or a vector that contained an exogenous signal peptide (Ig-like domain)[46]. Proteins were expressed as secreted proteins in HEK293E cells[47].

Expression cloning. The Izumo1 receptor was identified by an expression cloning method as described[48], using a normalized mouse oocyte cDNA library (NIH_MGC_257_N, Express Genomics, USA). Initial sequencing of randomly-selected clones confirmed that the library contained a good fraction of unique full-length cDNAs: 130/161 (81%) of randomly sequenced plasmids were unique, and 18% were full-length as determined by the presence of the start methionine and stop codon. The cDNA library was plated at a density of ~100 colonies per plate and pools of purified plasmids were transfected using Lipofectamine 2000 (Invitrogen) into HEK293T cells (ATCC catalogue no. CRL-3216) grown as adherent monolayers in flat-bottomed 48-well microtitre plates. After 48 h, cells were incubated with the Flag-tagged Izumo binding probe for 30 min, washed, fixed with a 4% formalin solution and stained with an anti-Flag Cy3 (Sigma). Wells were manually inspected for Izumo1 staining with an epifluorescence microscope and plasmid pools that resulted in positive Izumo1 staining were used to transform DH5α *Escherichia coli*. Plasmids were purified from individual colonies grown in 96-well blocks, pooled into groups of twelve, and HEK293T cells again transfected and tested for Izumo1 binding 48 h later as described above. A final round of Izumo1 staining was performed with individual plasmids from the positive pools to identify three independent positive clones which were sequenced using Sanger dideoxy sequencing to identify *Folr4*, which was renamed *Juno*.

Staining mouse eggs with avid recombinant proteins and antibodies. To detect the Izumo1 probe binding to the oolemma, purified pentamerized Flag-tagged Izumo1 was added to unfixed eggs. After 30 min at 37 °C, eggs were fixed with 2% formalin, washed, and stained with anti-Flag-Cy3 antibody diluted 1:500 in M2 medium. Izumo1 binding to HEK293T cells was detected using the same method, except that protein and antibody were diluted in PBS/2% BSA. Juno was detected on eggs fixed with 2% formalin using the anti-Juno/Folr4 monoclonal antibody diluted to 2 µg ml^{-1} in M2 medium, washed, followed by an anti-rat Alexa Fluor 488. Stained eggs were mounted on a microscope glass in SlowFade with DAPI (Molecular Probes). Samples were analysed with Leica SP5/DM6000 confocal microscope.

Extracellular protein interaction screening by AVEXIS. Bait and prey proteins were normalized to activities suitable for the AVEXIS assay as described[49]. Biotinylated baits that had been either purified or dialysed against HBS were immobilised in streptavidin-coated 96-well microtitre plates (NUNC). Preys were incubated for two hours, washed 3× HBS/0.1% Tween-20, 1× HBS and 125 µg ml^{-1} of nitrocefin added, and absorbance values measured at 485 nm on a Pherastar plus (BMG laboratories). A protein consisting of the rat CD4d3+4 tag alone was used as a negative control bait and a biotinylated anti-CD4 monoclonal antibody (anti-prey) used as a positive control as required. The mouse Izumo1–Juno interaction has been repeated more than three times in the laboratory by AVEXIS using independent protein preparations; importantly, the interaction is observed if the Izumo1 or Juno proteins are presented as either the bait or prey. Similarly, the Izumo1–Juno interactions from different mammalian species were repeatable and independent of the bait-prey orientation.

Antibodies. Antibodies were obtained from the following suppliers: mouse anti-rat CD4d3+4, clone OX68 (AbD Serotec), rat anti-mouse Folr4/Juno, clone TH6 (BioLegend), Armenian hamster anti-mouse CD55, clone RIKO-3 (BioLegend), rat anti-trinitrophenol+KLH IgG_{2b} isotype control (BioLegend), anti-Flag-Cy3 conjugated (Sigma), anti-rat AlexaFluor 488 and 568 (Molecular Probes), mouse anti-mouse Izumo1 OBF13 was a gift from N. Inoue and M. Okabe.

Surface plasmon resonance. Protein interactions were quantified by surface plasmon resonance studies as implemented in a Biacore T100 instrument (GE Healthcare). Briefly, biotinylated proteins were immobilised on a streptavidin-coated sensor chip. Approximately 450 RU of rat CD4d3+4 was used as a reference and approximate molar equivalents of biotinylated mouse Izumo1CD4d3+4 protein immobilised in the query flow cell. Purified mouse JunoCD4d3+4–6His protein was resolved by gel filtration just before SPR experiments to remove any aggregated protein which influence the measurement of kinetic parameters. Increasing concentrations of purified JunoCD4d3+4-6His was injected at 10 µl min^{-1} for equilibrium measurements whereas high flow rates (100 µl min^{-1}) were used for kinetic

measurements to reduce the confounding effects of analyte rebinding. Although essentially all the bound Juno dissociated during the wash-out phase, the surface was 'regenerated' with a pulse of 2 M NaCl at the end of each cycle. Equilibrium binding measurements were taken once equilibrium had been reached using reference-subtracted sensorgrams. Duplicate injections of the same concentration of Juno CD4d3+4–6His in each experiment were superimposable demonstrating no loss of activity after regenerating the surface. Both kinetic and equilibrium binding data were analysed in the manufacturer's Biacore T100 evaluation software (GE Healthcare) and all experiments were performed at 37 °C.

Enzyme-linked immunosorbent assay (ELISA) and western blotting. Biotinylated proteins were captured on streptavidin-coated plates for one hour before adding 10 μg ml^{-1} primary antibody for 90 min. Plates were washed in HBS/0.1% Tween-20 (HBST) before adding the appropriate secondary antibody conjugated to alkaline phosphatase (Sigma). Plates were washed 3× HBST and 1× HBS before adding 100 μl *p*-nitrophenyl phosphate (Sigma 104 alkaline phosphatase substrate) at 1 mg ml^{-1} in diethanolamine buffer. Absorbance readings were taken at 405 nm on a Pherastar plus (BMG laboratories). Where appropriate, proteins were denatured by heat treatment at 90 °C for 10 min. ELISAs were performed at room temperature.

Western blotting was performed essentially as described[50]. Briefly, secreted biotinylated Izumo1 domains were normalized and resolved under non-reducing conditions by SDS–PAGE and blotted to Hybond-P PVDF membrane (GE Healthcare) for 2 h at 30 V. After blocking for 1 h with 2% BSA, the membrane was incubated for 1 h with OBF13 diluted 1:200 in PBST/2% BSA, washed three times and incubated with an horseradish peroxidase (HRP)-conjugated anti-mouse antibody. Proteins were detected using SuperSignal West Pico Chemiluminescent substrate (Thermo Scientific).

Folate binding assays. Endogenous folate was first dissociated from its receptor and adsorbed to activated charcoal by incubating the biotinylated proteins for 20 min at 4 °C in 250 mM NaCl, 25 mM sodium acetate, 1% Triton X-100, 15% FBS and 40 mg ml^{-1} charcoal, pH 3.5 as described[20]. After centrifugation, the solution was adjusted to pH 7.4 and the proteins were captured on streptavidin-coated plates for one hour. Folic acid conjugated to HRP (C057 CalBioreagents, USA) was diluted 1:150 in 25 mM Tris pH 8.0, 150 mM NaCl, 0.1% Triton X-100, and incubated for 1 h. Finally, the plates were washed, 100 μl of Ultra-TMB substrate (Pierce Biotechnology) was added and absorbance readings were taken after 45 min.

PIPLC treatment. Zona-free metaphase-II eggs or HEK293 cells transfected with an expression construct encoding full length *Juno* were treated with PIPLC (Sigma) for 30 min at 37 °C in HTF medium, washed and fixed with a 2% formalin solution. The presence of Juno was determined using the anti-Juno/Folr4 antibody using either immunocytochemistry by confocal microscopy (eggs) or flow cytometry (transfected HEK cells) on a BD Biosciences LSR Fortessa cell analyser and data analysed using FACSDiva software.

Juno immunogold electron microscopy. Eggs were resuspended in a 4% paraformaldehyde/0.2% glutaraldehyde mixture in PBS for one hour (all steps at room temperature), washed three times in PBS, blocked with PBS/glycine followed by 5% fetal calf serum for 30 min and then incubated in rat anti-Juno for 1 h. After rinsing, the eggs were incubated with goat anti-rat secondary antibody conjugated to ultra-small (0.8 nm) gold particles for 30 min, washed, and fixed in 1.5% glutaraldehyde for 30 min, rinsed in distilled water and then signals amplified with a silver enhancing kit (Amersham IntenSE M) for 10 min. The eggs were post-fixed in 1% osmium tetroxide for 30 min, dehydrated in an ethanol series and embedded in TAAB resin. 60 nm ultrathin sections were cut on a Leica UC6 ultramicrotome, contrasted with uranyl acetate and lead citrate and examined on a 120 kV FEI Spirit Biotwin using a Tietz F4.15 CCD camera.

Cellular binding/fusion assay using ectopic expression. HEK293T cells were transfected with plasmids encoding mouse *Juno* (clone B2 from the cDNA library) or with GFP-tagged full-length mouse *Izumo1* (clone MG222708, Origene, USA) using Lipofectamine 2000 (Invitrogen) according to the manufacturer's protocol. The day after transfection, equal numbers of cells were mixed and examined for binding and fusion using confocal microscopy two and 24 h later. Izumo1 was detected by the GFP tag and Juno using the anti-Juno antibody by immunocytochemistry. Briefly, cells were incubated with anti-Juno antibody, diluted 1:200 in PBS/2% BSA, washed in PBS followed by anti-rat Alexa Fluor 568-conjugated secondary antibody (Molecular Probes). Finally, nuclei were stained with DAPI (Slow Fade mounting medium, Molecular Probes).

45. Martin, S. *et al.* Construction of a large extracellular protein interaction network and its resolution by spatiotemporal expression profiling. *Mol. Cell. Proteomics* **9,** 2654–2665 (2010).
46. Crosnier, C. *et al.* A library of functional recombinant cell-surface and secreted *P. falciparum* merozoite proteins. *Mol. Cell. Proteomics* **12,** 3976–3986 (2013).
47. Durocher, Y., Perret, S. & Kamen, A. High-level and high-throughput recombinant protein production by transient transfection of suspension-growing human 293-EBNA1 cells. *Nucleic Acids Res.* **30,** e9 (2002).
48. Golemis, E. A. & Adams, P. D. *Protein-Protein Interactions: A Molecular Cloning Manual.* (Cold Spring Harbor Laboratory Press, 2001).
49. Kerr, J. S. & Wright, G. J. Avidity-based extracellular interaction screening (AVEXIS) for the scalable detection of low-affinity extracellular receptor-ligand interactions. *J. Vis. Exp.* **61,** e3881 (2012).
50. Bartholdson, S. J. *et al.* Semaphorin-7A is an erythrocyte receptor for *P. falciparum* merozoite-specific TRAP homolog, MTRAP. *PLoS Pathog.* **8,** e1003031 (2012).

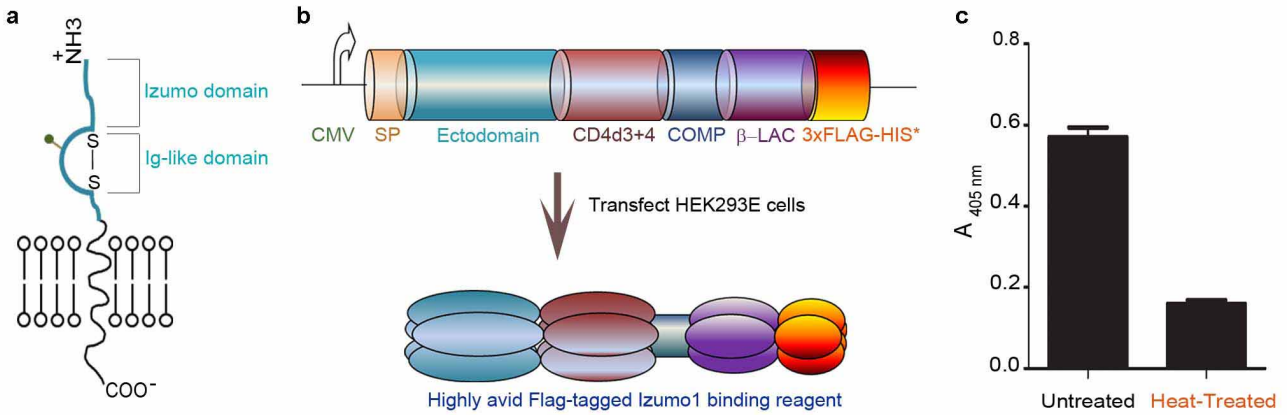

Extended Data Figure 1 | Expression of a soluble, biochemically active, highly avid recombinant mouse Izumo1 ectodomain. **a**, Schematic diagram of the mouse Izumo1 cell-surface protein as it would be displayed in the membrane. Izumo1 is a type I membrane protein containing an Ig-like domain predicted to contain a disulphide bond (S–S) and a single N-linked glycosylation site (filled lollipop). **b**, Diagram representing the plasmid encoding the highly avid, pentamerized Izumo1 ectodomain. The expression plasmid contains a cytomegalovirus (CMV) promoter driving the transcription of the entire ectodomain of mouse Izumo1 followed by the rat CD4 domains 3 and 4 tag, a region from the cartilage oligomeric matrix protein (COMP) that forms pentamers, a beta-lactamase (β-LAC) enzymatic tag, a 3×FLAG-tag for immunological detection and a C-terminal 6-HIS tag for purification. **c**, Immunoreactivity of the recombinant soluble mouse Izumo1 protein expressed as a biotinylated bait with the fertilization-blocking anti-Izumo1 monoclonal antibody OBF13, as assessed by ELISA. Untreated recombinant Izumo1 was highly immunoreactive, but this immunoreactivity was significantly reduced after heat treatment at 90 °C for 10 min, demonstrating the presence of a conformational heat-labile epitope. Bar graphs show mean ± s.e.m., $n = 3$.

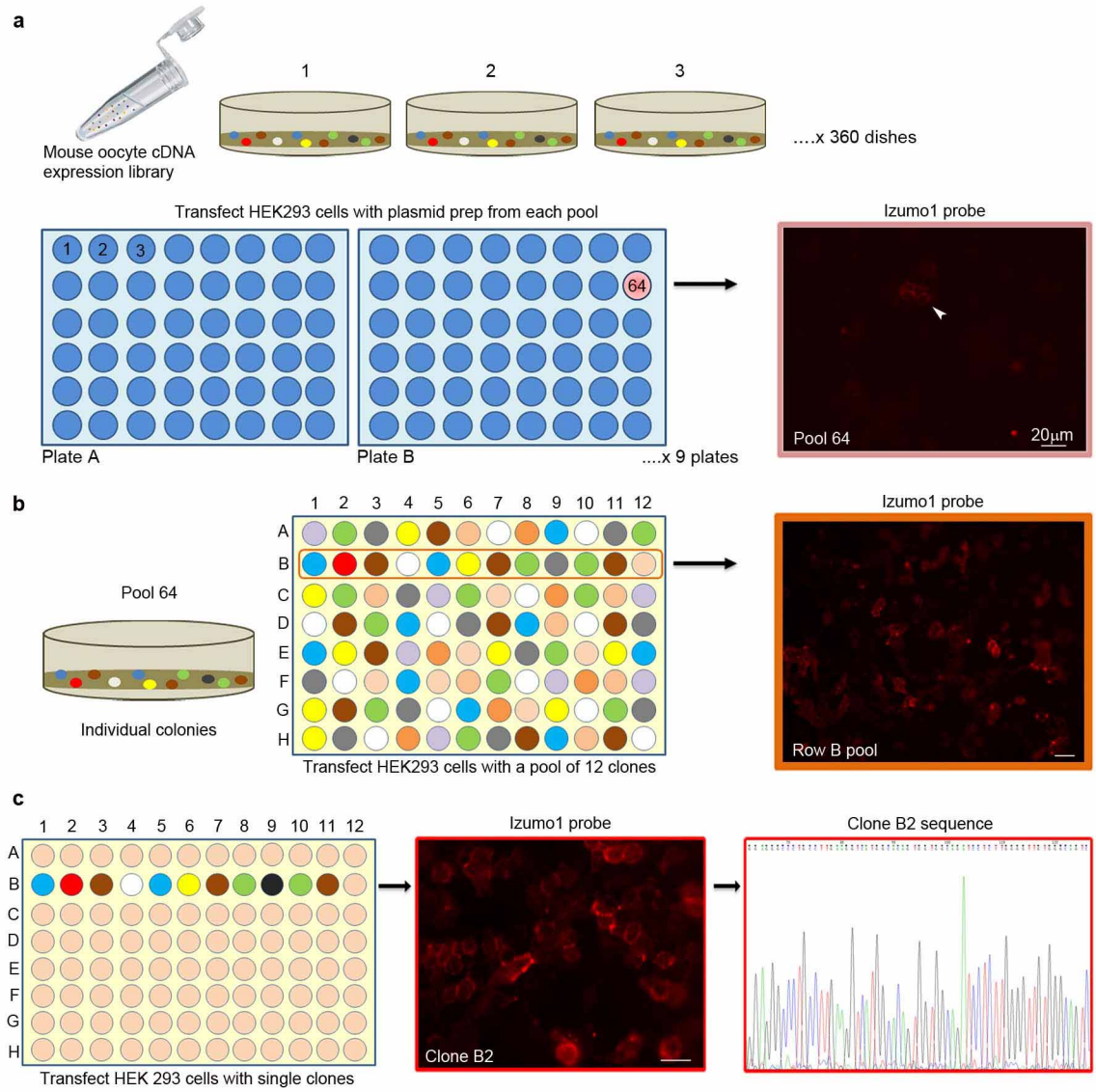

Extended Data Figure 2 | A schematic illustrating the expression cloning approach that identified Juno/Folr4 as an Izumo1 binding partner. **a**, A normalized mouse oocyte cDNA expression library was purchased as a glycerol stock from Express Genomics (MGC-257). The library was subsequently plated over 360 100-mm-diameter plates at a density of ~100 colonies per plate. The plasmids were purified as 360 pools from the colonies on each plate, and transfected into adherent HEK293T cells which were grown in 48-well microtitre plates and then tested for their ability to bind the recombinant Izumo1 probe using an anti-Flag-Cy3 secondary antibody followed by direct visual inspection. An example positive pool (pool 64) is shown—the arrowhead indicates a positively-stained cell. **b**, Pool 64 was retransformed and plasmids purified from 96 individual colonies. Further pools containing 12 colonies each were again transfected into HEK293 cells and assessed for Izumo1 binding; here, Row B contained a positive clone. **c**, Izumo1 staining of HEK293 cells transfected with individual plasmids from Row B identified clone B2 as encoding an Izumo binding partner which was then revealed as *Folr4/Juno* by sequencing and BLAST searching. Three individual plasmids were independently identified using this approach and all three contained an identical *Folr4/Juno* sequence.

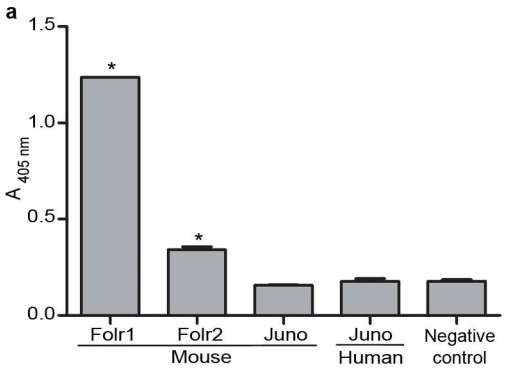

b

```
Folr1_human MAQRMTTQLLLLLVWVAVVGEAQTRIAWARTELLNVCMNAKHHKEKPGPEDKLHEQCRPWRKNACCSTNTS 71
Folr2_human MVWK-WMPLLLLLVCVATMC-----SAQDRTDLLNVCMDAKHHKTKPGPEDKLHDQCSPWKKNACCTASTS 65
 Juno_human MAC--WWPLLL-ELWT-------VMPTWAGDELLNICMNAKHHKRVPSPEDKLYEECIPWKDNACCTLTTS 61
Folr1_mouse MAHLMTVQLLLLLVMWMAEC--AQSRATRARTELLNVCMDAKHHKEKPGPEDNLHDQCSPWKTNSCCSTNTS 69
Folr2_mouse MAWK-QTPLLLLV-YMVTTG-----SGRDRTDLLNVCMDAKHHKTKPGPEDKLHDQCSPWKKNACCSVNTS 64
 Juno_mouse MAQ--WWQILL-GLWA-------VLPTLAGDKLLSVCMNSKRHKQEPGPEDELYQECRPWEDNACCTRSTS 61

QEAHKDVSYLYRFNWNHCGEMAPACKRHFIQDTCLYECSPNLGPWIQQVDQ-------SWRKERVLNVPLCKEDCEQWWEDC 146
QELHKDTSRLYNFNWDHCGKMEPACKRHFIQDTCLYECSPNLGPWIQQVNQ-------SWRKERFLDVPLCKEDCQRWWEDC 140
WEAHLDVSPLYNFSLFHCGLLMPGCRKHFIQAICFYECSPNLGPWIQPVGSLGWEVAPSGQGERVVNVPLCQEDCEEWWEDC 143
QEAHKDISYLYRFNWNHCGTMTSECKRHFIQDTCLYECSPNLGPWIQQVDQ-------SWRKERILDVPLCKEDCQQWWEDC 144
QELHKADSRLY-FNWDHCGKMEPACKSHFIQDSCLYECSPNLGPWIQQVDQ-------SWRKERFLDVPLCKEDCHQWWEAC 138
WEAHLEEPLLFNFSMMHCGLLTPACRKHFIQAICFHECSPNLGPWIQPVVPNG------QEEQRVWGVPLCQEDCEDWWRAC 137

RTSYTCKSNWHKGWNWTSGFNKCAVGAACQPFHFYFPTPTVLCNEIWTHSYKVSNYSRGSGRCIQMWFDPAQGNPNEEVARF 228
HTSHTCKSNWHRGWDWTSGVNKCPAGALCRTFESYFPTPAALCEGLWSHSYKVSNYSRGSGRCIQMWFDSAQGNPNEEVARF 222
RMSYTCKSNWRGGWDWSQGKNRCPKGAQCLPFSHYFPTPADLCEKTWSNSFKASPERRNSGRCLQKWFEPAQGNPNVAVARL 225
QSSFTCKSNWHKGWNWSSGHNECPVGASCHPFTFYFPTSAALCEEIWSHSYKLSNYSRGSGRCIQMWFDPAQGNPNEEVARF 226
RTSFTCKRDWHKGWDWSSGINKCPNTAPCHTFEYYFPTPASLCEGLWSHSYKVSNYSRGSGRCIQMWFDSTQGNPNEDVVKF 220
HSSLTCKSNWLHGWDWSEEKKHCPAHEPCLPFSYHFPTPDDLCEKIWNNTFKASPERRNSGRCLQKWFEPTLSNPNVEVALH 219

YAAAMSGAGP---WAAWPFLLSLALML-LWLLS 257
YAAAMHVNAGEMLHGTGGLLLSLALMLQLWLLG 255
FASSAPSWELSY---T-IMVCSLFLPF---LS- 250
YAEAMS---GAGLHGTWPLLCSLSLVL-LWVIS 255
YASFMT--SGTVPHAAVLLVPSLAPVLSLWLPG 251
FAGSALAPQLSY---T-LPAFSLCLLF---HP- 244
```

Extended Data Figure 3 | Juno/Folr4 does not bind folate, consistent with differences in amino acids known to be involved in folate binding. **a**, Soluble, biotinylated recombinant proteins corresponding to the entire ectodomains of mouse Folr1, Folr2 and Juno or human Juno were captured on a streptavidin-coated plate and washed. Folic acid binding was quantified relative to a CD200R negative control by adding a folic acid–HRP conjugate followed by an HRP substrate. Folic acid bound Folr1 and Folr2, but not mouse or human Juno. **b**, A multiple sequence alignment of human and mouse Folr1, Folr2 and Juno highlighting residues which are critical for folic acid binding. Sequences were aligned and structural features annotated: the signal peptide is in green, the GPI-anchor cleavage sites are underlined in bold for Folr1 and Folr2, and the best-scoring prediction is underlined pink for Juno. Residues located in the folic acid binding pocket and which affect folic acid binding are marked in red and differences highlighted in blue. Only 9 out of 15 residues involved in folic acid binding are conserved in human Juno relative to human Folr1, and 6 out of 15 are conserved in mouse Juno. Bar graphs represent mean ± s.e.m., $n = 3$. *One way ANOVA, $P < 0.05$ (Tukey's test).

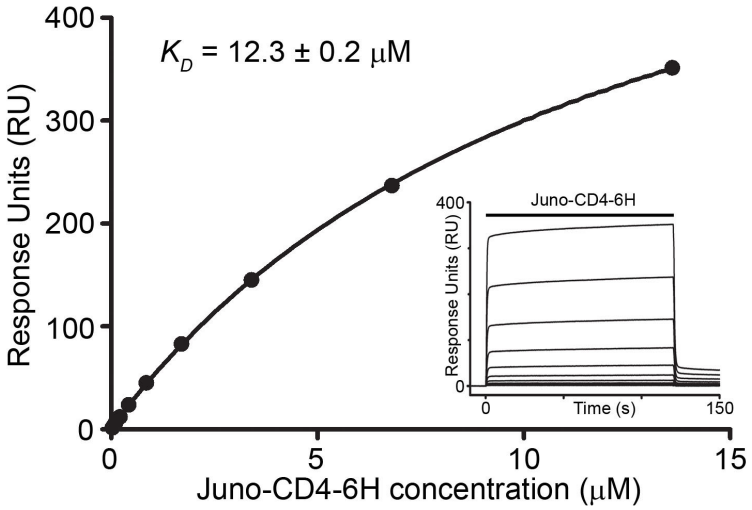

Extended Data Figure 4 | Mouse Izumo1 and Juno interact with a very low equilibrium binding constant. Serial twofold dilutions of purified and gel-filtrated JunoCD4d3+4–His were injected (solid bar, inset) through flow cells containing 450 RU CD4d3+4–bio (used as a reference) and 1,150 RU (approximate molar equivalent) of biotinylated Izumo1CD4d3+4 captured on a streptavidin-coated sensor chip. Binding after reference subtraction was quantified once equilibrium had been reached (see inset) and plotted as a binding curve (main figure). An equilibrium dissociation constant (K_D) was calculated using nonlinear regression fitting of a simple Langmuir binding isotherm to the data (solid line). The K_D of 12.3 ± 0.2 μM was in excellent agreement with independently obtained kinetic data ($K_{Dcalc} = k_d/k_a = 1.387\ s^{-1}/1.03 \times 10^5\ M^{-1}\ s^{-1} \approx 13.5\ \mu M$).

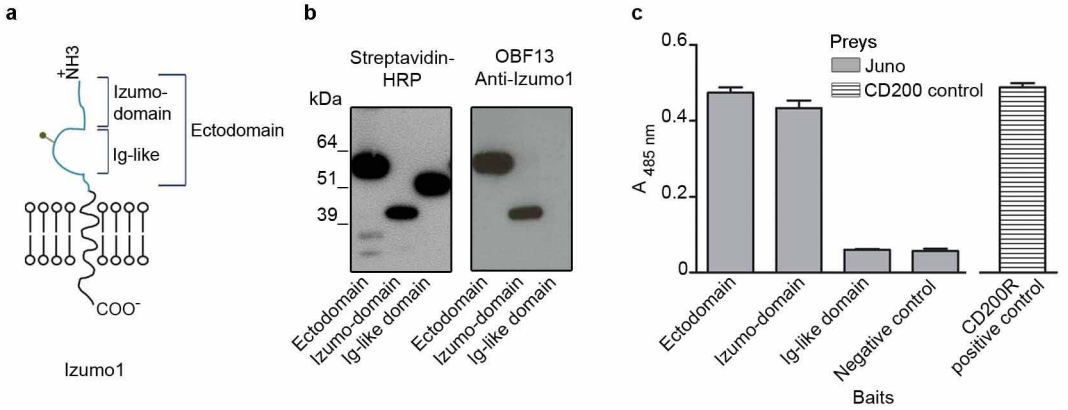

Extended Data Figure 5 | The N-terminal Izumo domain of Izumo1 contains both the anti-Izumo1 fertilization-blocking OBF13 monoclonal antibody epitope and the Juno binding site. **a**, Schematic representation of the Izumo1 protein. **b**, The entire ectodomain, the N-terminal Izumo domain and Ig-like domain of Izumo1 were expressed as soluble biotinylated proteins at the expected size as shown by western blotting under non-reducing conditions using streptavidin–HRP (left panel). Probing the blotted proteins with the anti-Izumo1 fertilization-blocking monoclonal antibody OBF13 (right panel) demonstrated that the OBF13 epitope was located in the N-terminal Izumo domain. **c**, The binding site for Juno was localized to the N-terminal Izumo domain by using the AVEXIS assay. AVEXIS is an approach designed to detect direct low-affinity extracellular interaction between recombinant proteins expressed as either monomeric biotinylated 'bait' proteins or pentameric enzyme-tagged 'prey' proteins. The biotinylated bait proteins were captured on a streptavidin-coated microtitre plate and probed for interactions with the Juno prey. Both the entire ectodomain and Izumo domain alone bound the Juno prey relative to the Ig-like domain or CD4 negative control. The CD200 (prey)–CD200R (bait) interactions was used as a positive control. Bar charts show mean ± s.e.m., $n = 3$.

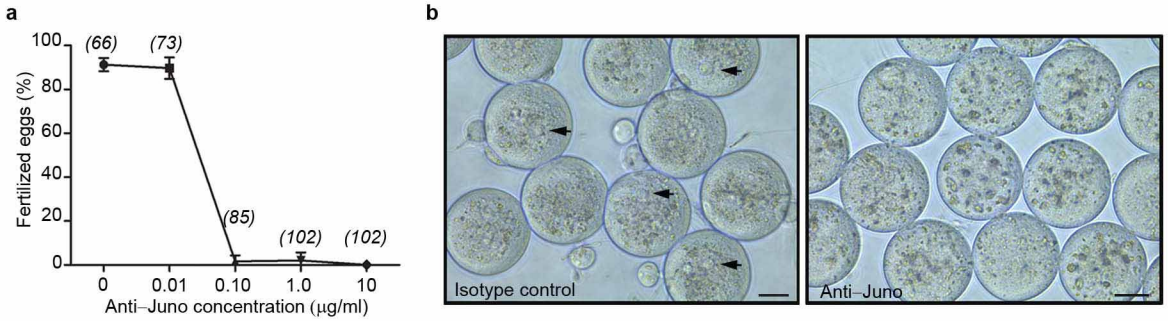

Extended Data Figure 6 | An anti-Juno/Folr4 antibody potently blocked fertilization in IVF assays. **a**, Titrating the dose of an anti-Juno monoclonal antibody in IVF assays showed that antibody concentrations of 0.1 μg ml^{-1} or above potently prevented fertilization. The numbers in parentheses report the total number of scored eggs from three independent experiments and fertilization was quantified by observing the presence of pronuclei six hours after addition of sperm. **b**, Images of the eggs at the end of the IVF assay performed in the presence of 10 μg ml^{-1} of either the isotype-matched control antibody (left image) or anti-Juno (right image). Pronuclei (arrows) and second polar body extrusion were clearly visible in the fertilized control eggs, but not in those incubated with the anti-Juno antibody. Scale bar, 20 μm.

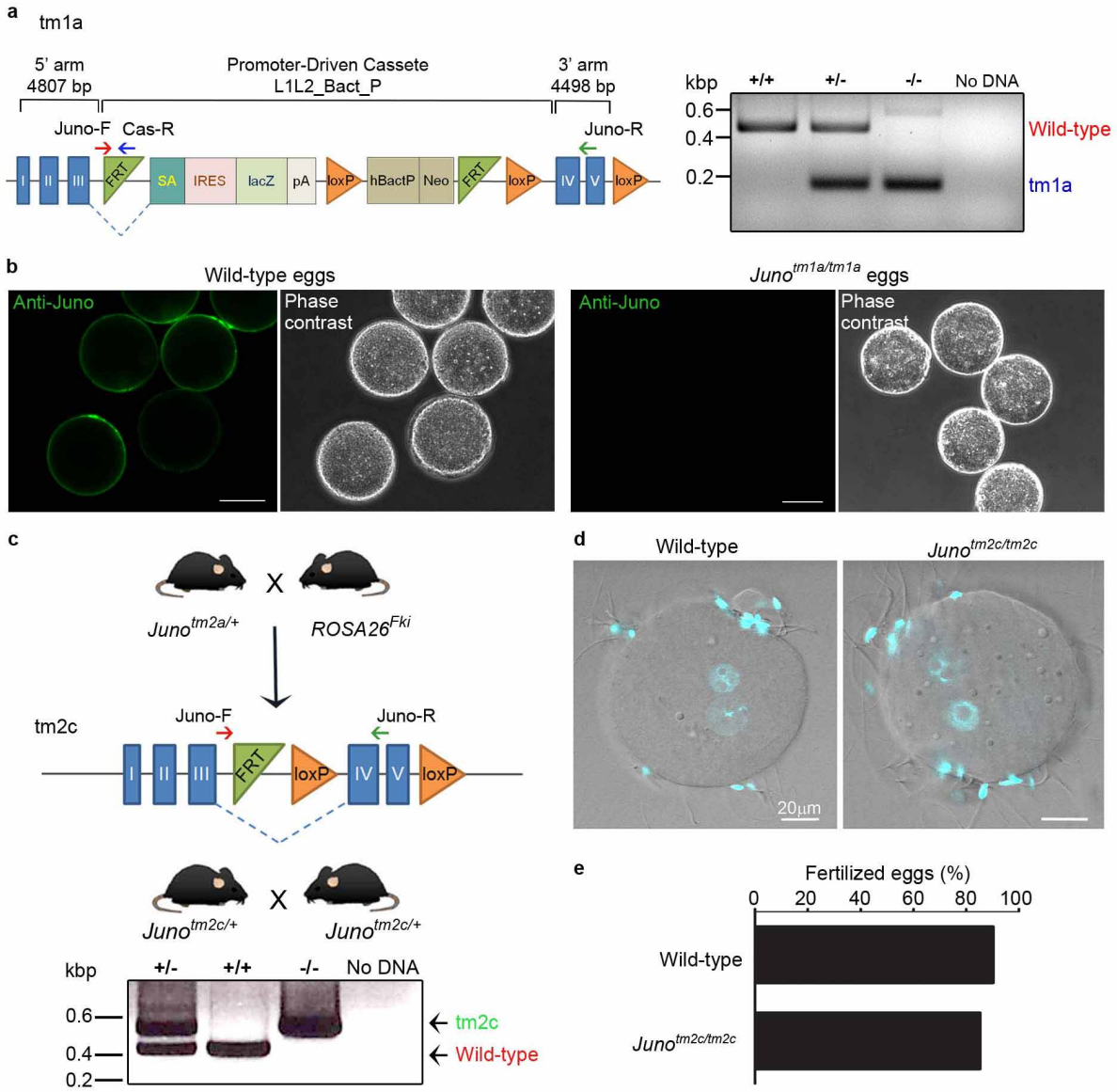

Extended Data Figure 7 | *Juno*-deficient mice: allele architecture, lack of detectable Juno on *Juno*$^{-/-}$ oocytes and fertility rescue with a genetic revertant. **a**, Juno-deficient mice were generated using embryonic stem cells targeted at the *Juno/Folr4* locus using a gene trapping cassette (*Folr4*$^{tm1a(KOMP)Wtsi}$) containing a strong splice acceptor site (SA) followed by an internal ribosome entry site (IRES), lacZ reporter and a polyadenylation site (pA) between *Juno* exons III and IV. Splicing from exon III of *Juno* to the transgene disrupts the *Juno* gene. FRT and loxP indicate recombinase recognition sites. Juno exons are indicated as blue boxes. Juno-F and Juno-R primers amplify a 440-bp PCR product from wild-type genomic DNA, and Juno-F and Cas-R primers amplify a 128-bp PCR product from the tm1a knockout (tm1a) or heterozygous mice. **b**, Eggs were collected from wild-type and *Juno*$^{tm1a/tm1a}$ mice and stained with an anti-Juno monoclonal antibody (green). Whereas Juno was highly expressed on eggs from wild-type mice, no Juno could be detected on eggs homozygous for the *Juno* tm1a allele. Scale bar, 50 µm. **c**, A second colony of *Juno*-deficient mice were created using an independent embryonic stem cell clone targeted with the same gene trapping allele (*Folr4*$^{tm2a(KOMP)Wtsi}$). The homozygous *Juno*$^{tm2a/tm2a}$ mutant females were also infertile, indicating that the infertility phenotype of *Juno*$^{tm1a/tm1a}$ females was not due to closely linked secondary mutations. To confirm this, the *Juno*^{tm2a} allele was reverted essentially to a wild-type 'floxed' *Juno*^{tm2c} allele by crossing heterozygous *Juno*$^{tm2a/+}$ mice to mice that constitutively and ubiquitously express the FLPe-recombinase from the *Rosa26* locus (*Rosa26*^{Fki} mice). Homozygous *Juno*$^{tm2c/tm2c}$ (indicated by −/−) female mice were obtained by breeding *Juno*$^{tm2c/+}$ heterozygotes and genotyped by PCR using the Juno-F and Juno-R primers; a representative PCR genotyping experiment is shown. **d**, **e**, Eggs from reverted *Juno*$^{tm2c/tm2c}$ mice are fertile. **d**, Image of a reverted *Juno*$^{tm2c/tm2c}$ egg fertilized by IVF relative to wild-type control. Successful fertilization is scored by the clear presence of pronuclei as detected by DNA staining (DAPI, blue). **e**, Quantification of the number of eggs fertilized by IVF from the reverted *Juno*$^{tm2c/tm2c}$ eggs relative to wild-type controls ($n = 40$ eggs from wild-type and $n = 20$ from *Juno*$^{tm2c/tm2c}$, collected from two mice).

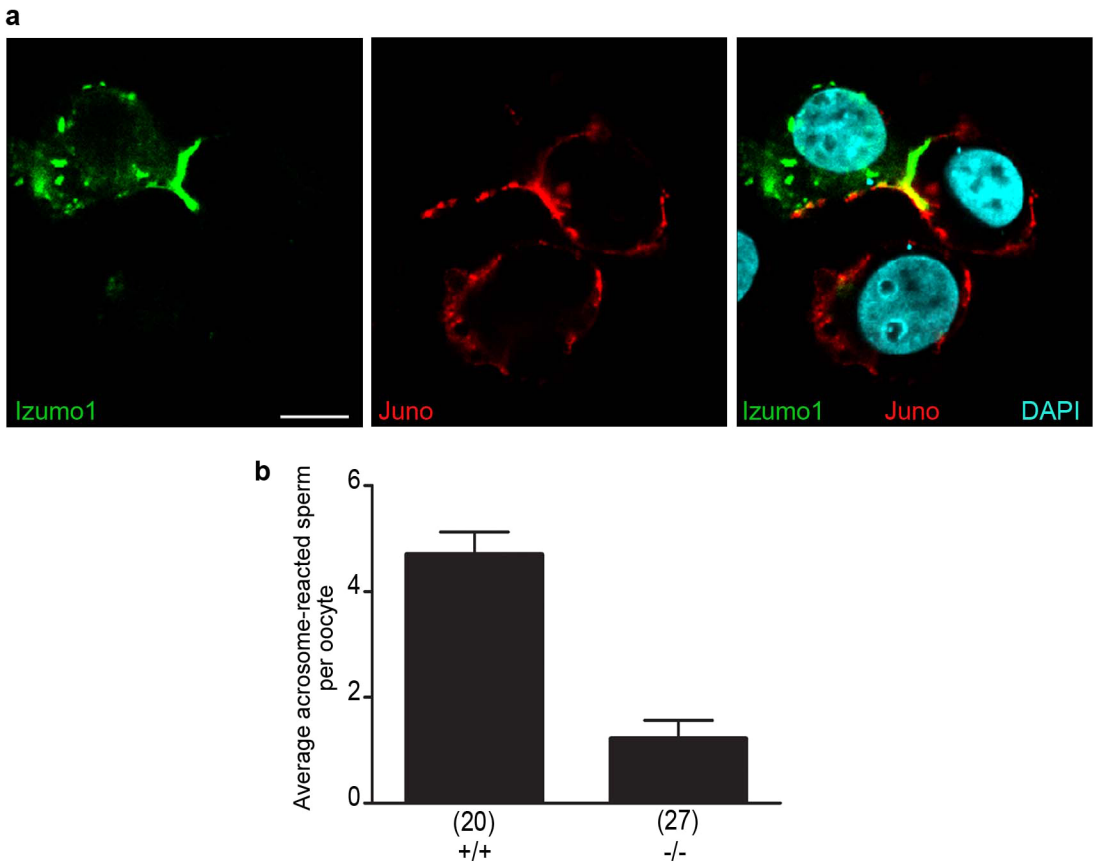

Extended Data Figure 8 | The Izumo1–Juno interaction is not sufficient for cell fusion but is required for efficient sperm–egg adhesion. **a**, HEK293T cells transfected with plasmids encoding either *Juno* or full-length, GFP-tagged *Izumo1* were mixed and cultured for 24 h before analysis by confocal microscopy. Izumo1 was detected by GFP fluorescence (green) and Juno using an anti-Juno antibody (red) and nuclei using DAPI (blue). No fused cells were observed, but both Izumo1 and Juno were enriched at sites of cellular contact. Scale bar, 10 μm. **b**, Sperm were collected from (B6;B6C3-Tg(Acro3-EGFP)01Osb) acrosome reporter mice and capacitated before mixing with zona-free eggs at a 1:70 egg:sperm ratio. Acrosome-reacted (GFP-negative) sperm bound less efficiently to *Juno*-deficient (−/−) than wild-type (+/+) control eggs. Bars represent mean ± s.e.m., the number of eggs is indicated in parentheses.

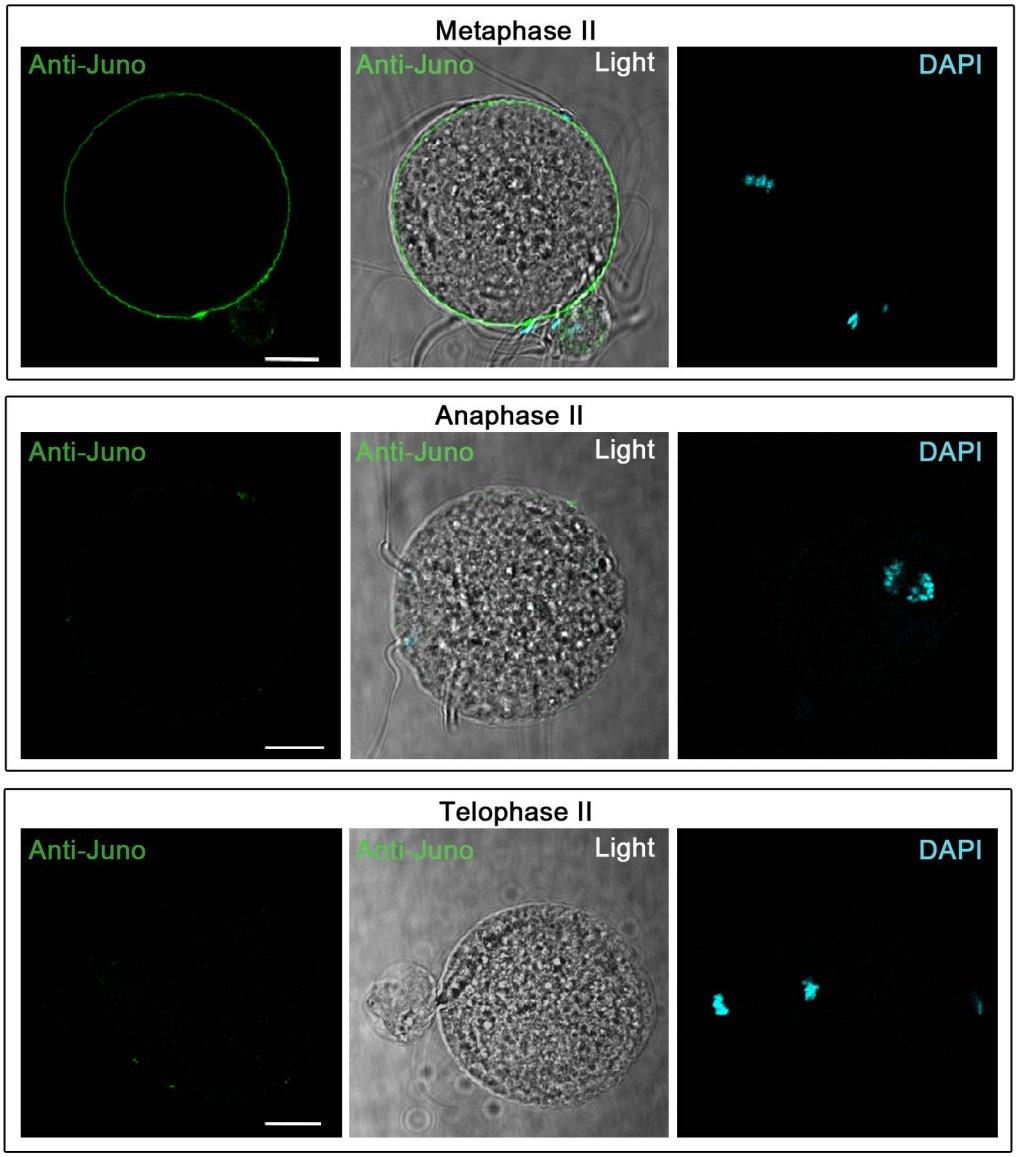

Extended Data Figure 9 | Juno staining is essentially undetectable on fertilized anaphase II zona-free eggs. Wild-type eggs were removed from IVF assays at different time points after addition of sperm, and Juno detected by confocal microscopy using an anti-Juno antibody (green); fertilized eggs were staged by the morphology of the chromosomes stained by DAPI (blue). Juno is highly expressed on the surface of metaphase II eggs (top panel), but is barely detectable by anaphase II (middle panel, approximately 45 min after fertilization), and late telophase II (bottom panel, approximately 60 min after fertilization). Scale bar, 20 μm. Note: DAPI images are taken from a different focal plane to clearly show chromosomes.